applied sciences

MDPI

Article

Improvement of Strength and Strain Characteristics of Lightweight Fiber Concrete by Electromagnetic Activation in a Vortex Layer Apparatus

Evgenii M. Shcherban' [1], Sergey A. Stel'makh [1], Alexey Beskopylny [2,*], Levon R. Mailyan [3], Besarion Meskhi [4] and Anatoly Shuyskiy [5]

1 Department of Engineering Geology, Bases, and Foundations, Don State Technical University, 344003 Rostov-on-Don, Russia; au-geen@mail.ru (E.M.S.); sergej.stelmax@mail.ru (S.A.S.)
2 Department of Transport Systems, Faculty of Roads and Transport Systems, Don State Technical University, 344003 Rostov-on-Don, Russia
3 Department of Roads, Don State Technical University, 344003 Rostov-on-Don, Russia; lrm@aaanet.ru
4 Department of Life Safety and Environmental Protection, Faculty of Life Safety and Environmental Engineering, Don State Technical University, 344003 Rostov-on-Don, Russia; reception@donstu.ru
5 Department of Technological Engineering and Expertise in the Construction Industry, Faculty of Civil Engineering, Don State Technical University, 344003 Rostov-on-Don, Russia; a2293613@mail.ru
* Correspondence: besk-an@yandex.ru; Tel.: +7-863-273-8454

Abstract: The relevant problem of choosing effective materials for enclosing structures is compliance with the requirements of increased thermal resistance, reduced mass of buildings and structures, and reduced material consumption, labor intensity, and construction costs. These requirements are satisfied by structures made of lightweight fiber-reinforced concrete, which are the subject of attention of many scientists and engineers. One of the most rational requirements for industrial use is the activation of untreated components of the concrete mixture. This article is devoted to studying the influence of the activation of fiber-reinforced concrete elements in the vortex layer apparatus on concrete strength and structural characteristics. The effect of the raw component processing time of the concrete mixture on the strength and deformation characteristics of the lightweight fiber-reinforced concrete was studied. The optimal processing time for the cement–sand mortar in the VLA-75-85s was determined. It was shown that the activation of the vortex layer in the apparatus leads to an increase in strength from 27% to 61% and an improvement in the deformation characteristics of lightweight fiber-reinforced concrete by up to 12%. Furthermore, it was found that the use of activation in VLA leads to an increase in the coefficient of constructive quality for all experimentally determined strength characteristics of lightweight fiber-reinforced concrete by up to 27%.

Keywords: concrete activation; electromagnetic activation; vortex layer apparatus; compressive strength; strain characteristics

Citation: Shcherban', E.M.; Stel'makh, S.A.; Beskopylny, A.; Mailyan, L.R.; Meskhi, B.; Shuyskiy, A. Improvement of Strength and Strain Characteristics of Lightweight Fiber Concrete by Electromagnetic Activation in a Vortex Layer Apparatus. *Appl. Sci.* **2022**, *12*, 104. https://doi.org/10.3390/app12010104

Academic Editor: Lorena Zichella

Received: 20 November 2021
Accepted: 21 December 2021
Published: 23 December 2021

1. Introduction

To implement the task of energy effectiveness and resource conservation in construction, the efforts of researchers and the entire construction complex were directed to the development and improvement of the production of efficient materials and structures. A practical material for enclosing structures should increase thermal resistance, decrease the mass of buildings and facilities, and reduce material consumption, labor intensity, and construction costs. These requirements are met in one way or another by structures made of lightweight fiber-reinforced concrete. However, the most rational requirements for industrial use are activation methods of raw concrete mix components, which imply recycling and final grinding of the original ingredients. This recycling process contributes to achieving sustainable development goals in the construction industry. In addition, some methods

and compositions increase the strength of lightweight fiber-reinforced concrete. However, the most rational for industrial use is activating the raw components of the mixture.

Chemical activation can effectively serve as a scope, allowing to obtain dense or lightweight concrete-like materials through the reuse of waste materials as secondary raw components. This is the case of the alkali-activation process, which can be used to activate mineral powders derived as by-products from the stone industry complex [1,2], clay brick wastes [3], ground granulated blast furnace slags [4], coal fly ashes [5], and a variety of other waste types. The good mechanical and physical–technical properties of the materials thus obtained make them particularly suitable to promote sustainability and boost the circular economy in the construction field. Since they are obtained by adding value to waste by-products, they can be viewed as materials with low environmental impact, and therefore they offer promising prospects for a circular economy.

An analysis of the effects that occur when using cement as the binder (i.e., as the main active component) shows that the initial components of cement, being discrete dispersed bodies with an extensive granulometry, have different surface energy and manifest it in different ways when interacting with water. Therefore, during the preparation of concrete, effects are manifested that ensure the chemical interaction of the finely dispersed phase with water and the involvement of cement in chemical interaction, which will be stronger, the larger the opened awakened active surface it has. For this, treatment is used that contributes to the size reduction of the cement grains, destruction of flocculation structures, and the formation of fresh developed and chemically active cement surfaces with high reactivity, which is called activation.

In current technological practice, three basic activation methods are used: chemical, physical, and mechanical.

Chemical activation for cement is based on the use of various surfactants (surfactants) as additives to the cementitious mix, contributing to their spontaneous dispersion in solutions, which increases the activity of interaction with water [6–10]. The effectiveness of surfactants in improving dispersion is also manifested with even finer materials than cement, such as carbon nanotube additives [11–13].

Physical activation is carried out by influencing the environment with various physical effects (thermal, magnetic, electrical, etc.). For example, heat treatment can be a means of regulating the interaction of water and cement [14–16]. An increase in temperature increases the penetrating ability of water molecules condensing on cement particles and creates conditions for their destruction at the weakest points as a result of an adsorption decrease in strength and the creation of new surfaces. Its low rate of flow limits the use of this activation method.

Presumably, when electric current acts on activated substances, each particle can be considered as an electric capacitor, on the surface of which packets of activated water molecules are associated. Changing the "capacities" of micro capacitors should increase the intensity of the interaction of cement with water. However, the use of this activation method is limited by the poor knowledge of this process concerning cement.

In the case of magnetic activation of a water-containing dispersed system, processes similar to those described above are assumed. The application of a magnetic field improves the adhesive properties of the system. However, there is an opinion that the effect of magnetic treatment is not always positive and depends both on the composition of water and on the magnetic field of the Earth [17,18].

Mechanical activation is considered to be one of the most efficient and affordable ways to process substances. Mechanical activation is carried out using special ball mills, vibratory mills or roller crushers. The activation of the binder can be performed "dry" or "wet". The essence of activation is to increase the specific surface area of materials with a simultaneous increase in surface energy, which increases the reactivity of the cement binder. The disadvantages of the dry method of activating cement include the processing time, which can reach several hours, the high energy consumption of the equipment and its low productivity, and the short terms and complexity of the activated cement storage [10,19–30].

The cavitation treatment of a cement–water suspension in thermodynamic or hydrodynamic disperser-activators (cavitators) built into the technological process of preparing concrete mixtures is more effective. The principle of operation of cavitation installations is to create, in a liquid medium passing through the working elements of the installation, the effects of hydrodynamic and acoustic cavitation when the arising ultrasonic acoustic vibrations disperse and activate material particles. Intense impact on the cement–water suspension of micro-shocks, cavitation ruptures, stretching and ultrasonic vibration leads to its heating, crushing of particles of the dispersed phase and the formation of stable activated suspensions [31,32].

For example, in [6], studies were carried out to assess the effect of mixing time on the mechanical properties of alkali-activated cement (AAC) with crushed granular blast furnace slag (slag) and fly ash (FA) in a 1:1 ratio. ASTM C305 stirring method was used as the main mixing method. In addition, the authors took into account the time and technology of mixing and the difference in the order of mixing the slag and fly ash [6].

In study [33], an activator, metakaolin, and microsilica were used as a complex additive to increase the activity of steel slag powder. Experimental results show that the compressive strength of the mortar can reach more than 85% of the control composition, while the flexural strength can reach more than 90% of the flexural strength of the control composition. Furthermore, the results show that the method proposed in the study can reduce the cost of binders [33].

In [17], the methods of laser holographic interferometry were used. Powder-activated concrete of the new generation in comparison with the materials of the old and transitional generations were considered as the studied ones. Using laser interferometry, it was found that the introduction of micro-silica, especially in combination with amorphous-active microsilica, significantly postpones the onset of microcracking in cement samples. A specimen based on a cement–sand mortar without fine fillers is characterized by a lower level of cracking, while with an increase in the load, the fracture of the specimen has a block character [17].

In work [7], the resistance of concrete mixtures, activated with alkalis, to aggressive media, which concrete may encounter during operation, was investigated. The results showed that the frost resistance and acid resistance of concrete activated with alkalis increase as the content of slag and activator increases [7].

The authors of [8] studied the possibility of using steel slag, which is a by-product of ferrous metallurgy, as a coarse aggregate in alkali-activated ash-and-slag concrete mixtures. An additional coarse aggregate, steel slag, was included in the optimized mixture by replacing natural coarse aggregates. The fatigue behavior of concrete mixes in bending was investigated [8,25,27,28].

In [19], an approach to determining the parameters of the macro kinetics of concrete setting through the kinetic characteristics of hardening at different temperatures was discussed. The activating nature of concrete hydration processes has been confirmed experimentally. Furthermore, a computer simulation of the formation of concrete strength made it possible to forecast the structure and properties of concrete at the early stages of hardening [19].

The authors of [9] studied the mechanical properties, shrinkage, and heat release of concrete using fly ash with a high calcium content as a binder with two alkaline activators: sodium silicate (Na_2SiO_3) and sodium hydroxide (NaOH). Compressive strength, modulus of elasticity, shrinkage, and heat release of concrete were studied depending on the ratio and concentration of alkaline activators [9,10,26,29,30].

Some of the most effective activators in terms of the degree of mechanical, electrochemical, and electromagnetic effects on the processed materials and in terms of specific energy intensity are electromagnetic devices of the vortex layer. Activation is carried out in installations where the components are processed in a working area made in the form of a pipe with a diameter of 60–150 mm with ferromagnetic particles (needles) placed in it. Under the influence of an external rotating electromagnetic field, the needles move along

the working area, colliding with the particles of the components placed there, mixing and grinding them. This generates the effects of acoustic waves, electrolysis, magnetostriction, mechanostriction, and cavitation with high specific power. Evaluation of the degree of influence of the parameters of electromagnetic activators on the properties of raw materials is a complex scientific and technical problem that requires a solution.

Earlier, in the works of domestic and foreign authors, various types of activation of compositions based on cement were considered, first of all, these are solutions and multiple types of concretes [1–21,23,31–33]. Undoubtedly, one of the most effective types of cement activation, and the most accessible, is mechanical activation, which can be carried out by grinding or re-grinding in various grinding devices, such as ball and planetary mills, including by means of electromagnetic action in vortex layer devices, which is shown in [31,34].

These works became the basis for our research, which differs from these studies in that, for the first time, such activation was applied to components intended for lightweight fiber-reinforced concrete.

The purpose of this study was to search for opportunities and test the results of fulfilling the hypothesis of improving the strength and deformative characteristics of lightweight fiber-reinforced concrete using an installation for processing materials and activating mixing processes with simultaneous grinding of the material and its electromagnetic processing.

For the first time, research has been carried out, and results have been obtained on the positive effect of activation by electromagnetic action using devices of a vortex layer of a cement–sand mortar intended for lightweight fiber-reinforced concrete. Compositions were selected and substantiated, recommended for use in practice, the process was considered and studied from the point of view of physics that occurs during the specified process. An increase in strength and an improvement in deformative characteristics of lightweight fiber-reinforced concrete due to the applied activation has been substantiated.

2. Materials and Methods

2.1. Materials

During the research, no-additive Portland cement of the PC 500 D0 brand was used, the physical and mechanical characteristics and chemical composition of which are presented in Table 1.

Crushed granite was used as a coarse dense aggregate, and slag pumice was used as a porous one. Physical and mechanical characteristics of a large dense and porous aggregate are presented in Tables 2 and 3.

Quartz sand was used as a fine aggregate, the physical characteristics are presented in Table 4.

Basalt fiber was used as dispersed reinforcement. Table 5 shows the physical and mechanical characteristics of the fiber used.

As a control composition, heavy concrete of class B30 was designed with a workability of the mixture corresponding to a cone draft of 1–4 cm. The content of coarse aggregate fractions is represented by the following ratio: 60% fraction 10–20 mm; 40% fraction 5–10 mm [35,36]. The parameters of the composition of the concrete mixture obtained as a result of calculations are reflected in Table 6.

In the manufacture of lightweight fiber-reinforced concrete, part of the volume of dense aggregate was replaced with the same volume of porous in an amount of 30%. Basalt fiber was introduced in the amount of 3% by the weight of the cement. The water consumption was adjusted until the required concrete mix mobility was obtained [36].

Table 1. Physical and mechanical characteristics of Portland cement PC 500 D0 and its chemical composition.

Indicator Title	Value
Physical and mechanical	
Compressive strength at the age of 28 days, MPa	54.8
Setting time, min	
- start	155
- the end	220
The fineness of grinding, passage through a sieve No. 008,%	96.7
Specific surface, m^2/kg	2930
Normal density of cement paste,%	23.5
Chemical	
Weight loss on ignition,%	0.7
Silicon oxide content (SiO_2), %	20.89
Aluminum oxide content (Al_2O_3), %	4.72
Iron oxide content, (Fe_2O_3), %	4.32
Calcium oxide content (CaO), %	63.27
Magnesium oxide (MgO), wt %	2.362
Sulfuric acid anhydride (SO_3), wt %	2.81
Alkaline oxides in terms of Na_2O, wt %	0.69
Free calcium oxide content (CaO_{fr}), %	0
Chloride ion (Cl^-), wt %	0.038
Insoluble residue, %	0.2

Table 2. Physical and mechanical characteristics of crushed granite.

Fraction, mm	Bulk Density, kg/m^3	True Density, kg/m^3	Crushing, wt %	Content of Lamellar and Needle-Shaped Grains, wt %	Voidness, %
5–20	1437	2620	11.4	8.1	45

Table 3. Physical and mechanical characteristics of slag pumice.

Fraction, mm	Bulk Density, kg/m^3	True Density, kg/m^3	Strength by GOST 32496-2013, MPa	Voidness, %
5–20	612	1310	0.8	53

Table 4. Physical characteristics of dense fine aggregate.

Grain Composition							Passing through a Sieve No 0.16, wt %	Fineness Modulus	Content of Dust and Clay Particles, %	True Density, g/cm^3	Bulk Density, kg/m^3
Sieve Size, mm											
Partial and Full Sieve Rest, %											
10	5	2.5	1.25	0.63	0.315	0.16					
0	0	0.17	1.39	8.86	45.80	41.03	2.49	1.66	1.1	2650	1438
		0.17	1.56	10.42	56.21	97.25	99.74				

Table 5. Physical and mechanical properties of fiber.

Basalt Fiber	Tensile Strength, MPa	Fiber Diameter, mm	Fiber Length, mm	Elasticity Modulus, GPa	Density, kg/m^3	Elongation Coefficient, %
	3200	16×10^{-6}	12	80	2600	3.2

Table 6. Parameters of the composition of the concrete mixture.

Indicator Title	W/C	C, kg/m^3	W, L/m^3	CS, kg/m^3	S, kg/m^3	ρ_{cm}, kg/m^3
Indicator value	0.58	327	190	1315	573	2405

2.2. Methods

Mechanical activation of Portland cement and cement–sand mortar was carried out in an installation for processing materials and activating mixing processes with simultaneous grinding of the material and its electromagnetic treatment with VLA [34]. The general view of the installation of the VLA of an industrial design is shown in Figure 1, and the technical characteristics of the VLA are presented in Table 7. Externally, the apparatus is an inductor placed in a case. A pipe made of non-magnetic material (working space) passes through the bore of the inductor. When electricity is supplied, a powerful rotating electromagnetic field is created in the working space, which rotates the ferromagnetic elements placed in it. The latter become magnets and interact with the main field. As a result of the interaction, a number of effects are generated that affect the substance placed in the workspace. These effects can include-magnetostriction, mechanostriction, cavitation, electrolysis, torsion fields, acoustic waves. The specific power of these effects is high. The consequence of this is considerable increases in the rates of physicochemical processes in substances placed in the working space of the installation. The methods pass from the diffusion to the kinetic level, and as a result of the opening of chemical radicals, the reaction rates increase hundreds of times.

(**a**) (**b**)

Figure 1. General view of the VLA installation: (**a**) installation in a protective case, connected to the water supply; (**b**) installation without a protective case, not connected to the water supply.

The mechanical activation process is carried out as follows. A chiller is fed into the unit's cooling system, then power is applied, and processing begins. Previously, ferromagnetic needles with a length of 20 ± 2 mm are loaded into the working area, the diameter (d) of which is related to the length (l) in a ratio of 1:10 (l/d = 10). This ratio is optimal for the activation of cement in terms of impact efficiency and is selected empirically.

Table 7. Technical characteristics of the VLA.

Indicator Title	Indicator Value
Productiveness:	
- by water	10 m^3/hour
- by dry components	2 m^3/hour
Power consumption	2 kW
Weight of ferromagnetic needles in the working chamber	550 ± 10 g
The ratio of the mass of the processed product to the mass of ferromagnetic needles	from 1:1.08 to 1:1.12
Sizes	1600 × 600 × 1400 mm
Mass	250 kg

It is known that the greatest dispersing effect is obtained with wet grinding, i.e., in the aquatic environment. This is due to the wedging effect of water molecules entering the pores and cracks of the solid. Therefore, when carrying out the study, we used grinding of components in an aqueous medium in the form of cement suspensions or solutions.

At the first stage, studies of the dispersion characteristics of the cement paste processed in the VLA installation were carried out. In the experiment, the processing time of the cement paste in the VLA was varied in the range from 0 to 150 s. At the same time, the characteristics of the granulometric composition and the specific surface area of the cement particles were monitored. For particle size analysis, a Microsizer 201C laser particle analyzer was used. It is a fully automated device and is designed for fast and accurate measurement of particle size distribution in the range 0.2–600 µm. The general view of the device is shown in Figure 2, and its technical characteristics are shown in Table 8.

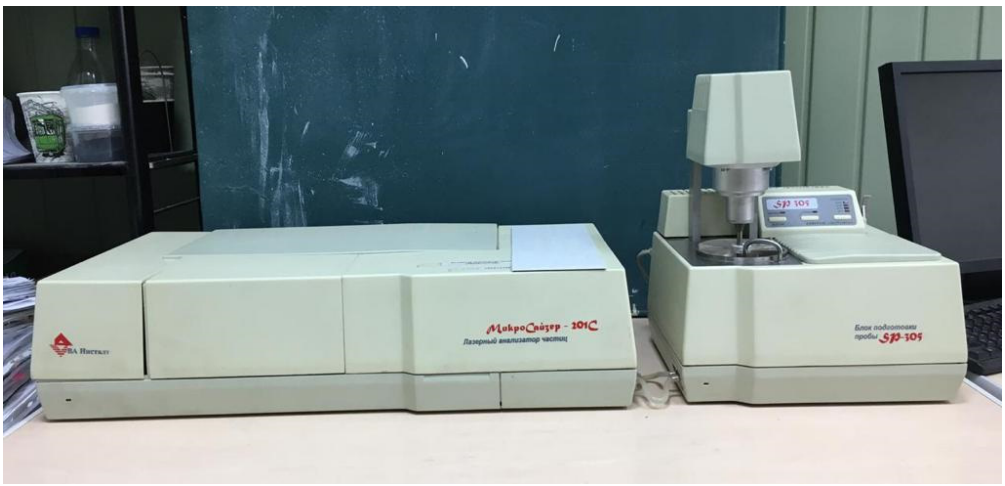

Figure 2. Laser particle analyzer Microsizer 201C.

Table 8. Technical characteristics of Microsizer 201C.

Indicator Title	Units	Value
Particle size range	µm	0.2–600
Radiation source		He–Ne laser
Detector		Photodiode Array
Number of registration channels	pieces	38
Sample preparation system		Ultrasonic Disperser
Sample chamber volume	mL	50
Ultrasonic frequency	kHz	50
Ultrasonic power	W	Up to 200

The PSKh-11 MSP device was used to control the specific surface area of the cement particles. The general view of the device is shown in Figure 3, and its technical characteristics are shown in Table 9.

Figure 3. Device for measuring the specific surface area of particles PSKh-11 MSP.

Table 9. Technical characteristics of PSKh-11 MSP.

Indicator Title	Indicator Value
Measured value range:	
- specific surface area, cm^2/g	300–500,000
- mass average particle size of powders, μm	0.5–300
Average measurement error, %	±10
Power consumption (220 V/50 Hz), less, W	30
Operating temperature range, °C	5–45
Sizes, mm	220 × 230 × 100

After processing in the VLA, 3 parts of standard sand (based on the mass of cement) were added to the resulting mixture, the mass was mixed in a laboratory concrete mixer for three minutes. Further, beams of a standard size (40 × 40 × 160 mm) were molded from the obtained cement–sand mortar. In total, 4 series of beams were made, 3 samples each. The samples hardened within 28 days under normal conditions (with a temperature of (20 ± 2) °C and a relative humidity of (95 ± 5)%). After that, the samples were subjected to physical and mechanical tests [37,38].

At the second stage, the cement–sand mortar was processed in the VLA. Then the activated cement–sand mortar was mixed with aggregates and fibers in a laboratory concrete mixer for three minutes. Further, from the resulting concrete mixture were made:

- sample—cubes with a size of 100 × 100 × 100 mm to determine the cube compressive strength (Figure 4);
- sample—prisms with a size of 100 × 100 × 400 mm to determine the prismatic compressive strength;
- sample—prisms with a size of 100 × 100 × 400 mm to determine the tensile strength in bending;

- sample—prisms with a size of 100 × 100 × 400 mm to determine the axial tensile strength.

Figure 4. Sample after compression test.

A total of 8 series were made, 3 samples each. The samples hardened within 28 days under normal conditions (with a temperature of (20 ± 2) °C and a relative humidity of (95 ± 5)%). After that, the samples were subjected to physical and mechanical tests.

The study also applied:

- technological equipment—laboratory concrete mixer BL-10 (ZZBO LLC, Chelyabinsk region, Zlatoust, Russia);
- testing equipment—hydraulic press IP-1000 (OOO NPK TEKHMASH, Neftekamsk, Republic of Bashkortostan, Russia), tensile testing machine R-50 (OOO IMash, Armavir, Russia);
- measuring instruments—measuring metal ruler 500 mm; laboratory scales; device for measuring deviations from the plane NPL-1; device for measuring deviations from perpendicularity NPR-1.

Compression, axial tensile and flexural tensile tests were carried out in accordance with the requirements of GOST 10180 "Concretes. Methods for strength determination using reference specimens" [39].

Axial compression tests were carried out in accordance with the requirements of GOST 24452 "Concretes. Methods of prismatic, compressive strength, modulus of elasticity and Poisson's ratio determination" [40].

Measurements of the concrete deformations of the test prisms were carried out by a chain of strain gauges with a side length of 50 mm and dial indicators with a graduation rate of 0.001 mm.

Additionally, for each type of strength, the values of the structural quality coefficients (*CCQ*) were calculated:

$$CCQ_{R_{b,cub}} = \frac{R_{b,cub}}{\rho}, \quad (1)$$

where $R_{b,cub}$ is cube compressive strength, MPa; ρ is concrete density, g/cm^3.

$$CCQ_{R_b} = \frac{R_b}{\rho}, \quad (2)$$

where R_b is prismatic compressive strength, MPa.

$$CCQ_{R_{btb}} = \frac{R_{btb}}{\rho}, \quad (3)$$

where R_{btb} is tensile strength in bending, MPa.

$$CCQ_{R_{bt}} = \frac{R_{bt}}{\rho}, \quad (4)$$

where R_{bt} is tensile strength, MPa.

3. Results and Discussion

3.1. Results of the Effect of Processing Cement and Cement Paste in the VLA on the Compressive Strength of Cement–Sand Mortar

The results obtained as a result of the first stage of research are presented in Table 10 and Figure 5.

Table 10. Influence of the processing time of cement in the VLA on its specific surface.

Composition Number	Processing Time in VLA, s	The Specific Surface Area of Cement Particles, cm^2/g
1	0	2930
2	50	3518
3	100	3740
4	150	4980

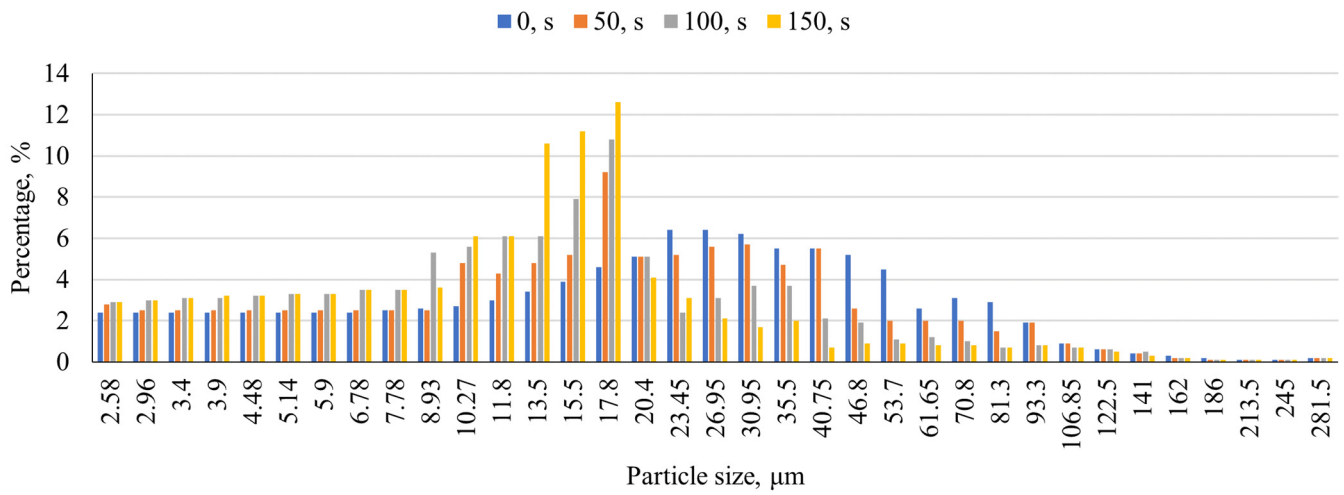

Figure 5. Dependence of the distribution of cement particles by fractions with a change in the processing time of cement in the VLA.

Analysis of the data obtained shows that an increase in the processing time of cement leads to an increase in its fine fractions. Thus, for untreated cement, the number of particles with a diameter of up to 20 microns is 42%, and for cement treated for 150 s—79%. The dependence of the specific surface area of cement on the duration of its processing in the VLA is presented in Table 10.

These changes in the dispersion of cement lead to an increase in the strength of the cement–sand mortar (CSM), which is confirmed by the test results of beam specimens given in Table 11, where the compressive strength is expressed in terms of average value ± the standard deviation.

Table 11. Influence of the processing time of the cement paste in the VLA on the growth of the strength of the cement–sand mortar samples and the specific surface area of cement particles.

Composition Number	Processing Time in VLA, s	Compressive Strength CSM, MPa
1	0	54.8 ± 3.4
2	50	65.1 ± 4.0
3	100	69.5 ± 4.3
4	150	53.9 ± 3.3

After analyzing the results obtained, it was found that when processing the cement paste in the VLA for 100 s, the maximum increase in the strength of the hardened cement–sand mortar is observed. Thus, the increase in the strength during processing for 100 s was 27%. However, with an increase in the processing time to 150 s, an adverse effect is observed. It is known that the activity of cement depends on the degree of its dispersion. With an increase in the specific surface area of cement, its strength characteristics increase. However, at the same time, water demand also increases, which negatively affects the strength characteristics of the binder. When the values of the specific surface area are close to 5000 cm^2/g, the negative effect of the increase in water demand is significant, making further cement grinding impractical. Based on the results obtained, it was decided to activate the cement–sand mortar for 0 (control point), 50, 60, 70, 80, 90, 100 s.

3.2. Influence of the Processing of Cement–Sand Mortar in the VLA on the Strength and Strain Characteristics of Lightweight Fiber-Reinforced Concrete

The results obtained as a result of the second stage of research are presented in Table 12 (where the experimentally determined values of all the mechanical characteristics are expressed as average value ± the standard deviation) and Figure 6.

Table 12. Influence of the processing time in the VLA of the cement–sand mortar on the growth of strength of lightweight fiber-reinforced concrete specimens.

Concrete Characteristics	Heavy Non-Activated Concrete	Lightweight Fiber Concrete						
		Processing Time in VLA, s						
		0	50	60	70	80	90	100
Density, kg/m^3	2439 ± 110	2080 ± 94	2087 ± 94	2097 ± 94	2089 ± 94	2091 ± 94	2095 ± 94	2086 ± 94
Cubic compressive strength, MPa	61.1 ± 3.9	43.2 ± 2.8	45.1 ± 2.9	49.2 ± 3.2	52.3 ± 3.4	54.7 ± 3.6	52.8 ± 3.4	50.3 ± 3.3
Prismatic compressive strength, MPa	45.8 ± 2.8	32.1 ± 2.0	34.8 ± 2.1	36.9 ± 2.3	39.2 ± 2.4	41.0 ± 2.5	39.6 ± 2.4	37.2 ± 2.3
Tensile strength in bending, MPa	11.0 ± 0.8	7.0 ± 0.5	8.1 ± 0.6	8.9 ± 0.6	9.4 ± 0.6	11.3 ± 0.8	10.1 ± 0.7	9.9 ± 0.7
Axial tensile strength, MPa	6.7 ± 0.4	5.0 ± 0.3	5.1 ± 0.3	5.4 ± 0.3	5.8 ± 0.3	6.6 ± 0.4	6.1 ± 0.4	5.8 ± 0.3
Ultimate deformations during axial compression, $mm/m \times 10^{-3}$	2.23 ± 0.12	2.89 ± 0.16	2.89 ± 0.16	2.97 ± 0.16	2.98 ± 0.16	3.08 ± 0.17	3.01 ± 0.17	3.01 ± 0.17
Ultimate deformations under axial tension, $mm/m \times 10^{-4}$	4.65 ± 0.28	4.86 ± 0.29	4.89 ± 0.29	4.86 ± 0.29	4.97 ± 0.30	5.31 ± 0.32	5.09 ± 0.31	5.02 ± 0.30
Elasticity modulus, GPa	36.3 ± 2.0	31.3 ± 1.7	32.5 ± 1.8	33.2 ± 1.8	33.6 ± 1.8	35.1 ± 1.9	34.7 ± 1.9	33.5 ± 1.8

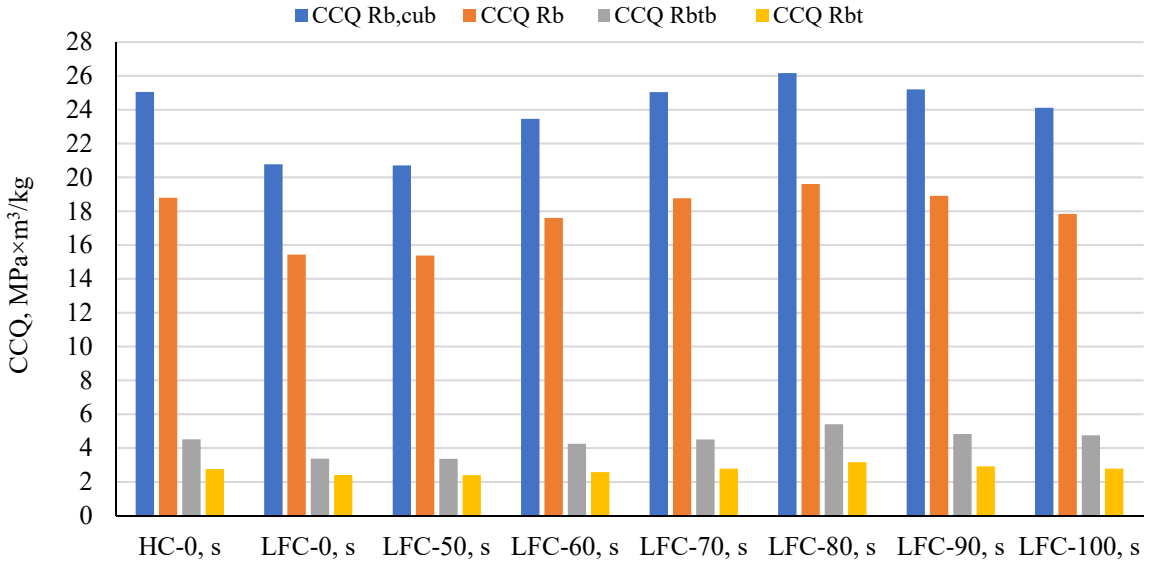

Figure 6. Influence of the processing time of the cement–sand mortar in the VLA on the coefficients of the constructive quality of lightweight fiber-reinforced concrete.

After analyzing the obtained experimental data on the effect of processing time on the strength and deformation characteristics of lightweight fiber-reinforced concrete, the following was established:

- when processing a cement–sand mortar for 50 s, the value of the increase in cubic strength in compression was 4%; prismatic compression strength 8%; tensile strength in bending 16%; axial tensile strength 2%; ultimate deformations during axial compression did not change; ultimate deformations under axial tension increased by 1%; the value of the elastic modulus increased by 4%;
- when processing a cement–sand mortar for 60 s, the value of the increase in cubic strength in compression was 14%; prismatic compression strength 15%; tensile strength in bending 27%; axial tensile strength 16%; ultimate deformations during axial compression increased by 3%; ultimate deformations under axial tension did not change; the value of the elastic modulus increased by 7%;
- when processing a cement–sand mortar for 70 s, the value of the increase in cubic strength in compression was 21%; prismatic compression strength 22%; bending tensile strength 34%; axial tensile strength 16%; ultimate deformations during axial compression increased by 3%; ultimate deformations under axial tension increased by 2%; the value of the elastic modulus increased by 7%;
- when processing a cement–sand mortar for 80 s, the value of the increase in cubic strength in compression was 27%; prismatic compression strength 28%; tensile strength in bending 61%; axial tensile strength 32%; ultimate deformations during axial compression increased by 7%; ultimate deformations under axial tension increased by 9%; the value of the elastic modulus increased by 12%;
- when processing a cement–sand mortar for 90 s, the value of the increase in cubic strength in compression was 22%; prismatic compression strength 23%; tensile strength in bending 44%; axial tensile strength 22%; ultimate deformations during axial compression increased by 4%; ultimate deformations under axial tension increased by 5%; the value of the elastic modulus increased by 11%;
- when processing a cement–sand mortar for 100 s, the value of the increase in cubic strength in compression was 16%; prismatic compression strength 15%; tensile strength in bending 41%; axial tensile strength 16%; ultimate deformations during axial compression increased by 4%; ultimate deformations under axial tension increased by 3%; the value of the modulus of elasticity increased by 7%.

Figure 6 shows that the maximum values of the structural quality coefficients, calculated for various types of strength, are observed in lightweight fiber-reinforced concrete made using a cement–sand mortar, activated in the VLA for 80 s.

Figures 7–13 show the correlation between the processing time in the VLA and cubic compressive strength, prismatic compression strength, tensile flexural strength, axial tensile strength, ultimate deformations in axial compression and axial tension of lightweight fiber-reinforced concrete, obtained as a result of the presented experimental research. The polynomial Equations (5)–(11), obtained by interpolating the experimental data, show the relationship between the processing time in the VLA (t) and the strength and deformation characteristics of lightweight fiber-reinforced concrete ($R_{b,cub}$, R_b, R_{btb}, R_{bt}, ε_b, ε_{bt}, E) together with the coefficient of determination (R^2):

$$R_{b,cub} = (-8E-5)\,t^3 + 0.0089t^2 + 0.1978t + 23.146,\ R^2 = 0.9839 \quad (5)$$

$$R_b = (-1.0E-4)t^3 + 0.0027t^2 + 0.1077t + 48.033,\ R^2 = 0.9804 \quad (6)$$

$$R_{btb} = -0.0021t^2 + 0.3575t - 4.728,\ R^2 = 0.7758 \quad (7)$$

$$R_{bt} = -0.012t^2 + 0.1951t - 1.8571,\ R^2 = 0.7998 \quad (8)$$

$$\varepsilon_b = -0.0001t^2 + 0.0216t + 2.1286,\ R^2 = 0.8133 \quad (9)$$

$$\varepsilon_{bt} = (-2E-5)t^3 + 0.0046t^2 - 0.3061t + 11.465,\ R^2 = 0.7297 \quad (10)$$

$$E = -0.0001t^3 + 0.0217t^2 - 1.3715t + 60.203,\ R^2 = 0.938 \quad (11)$$

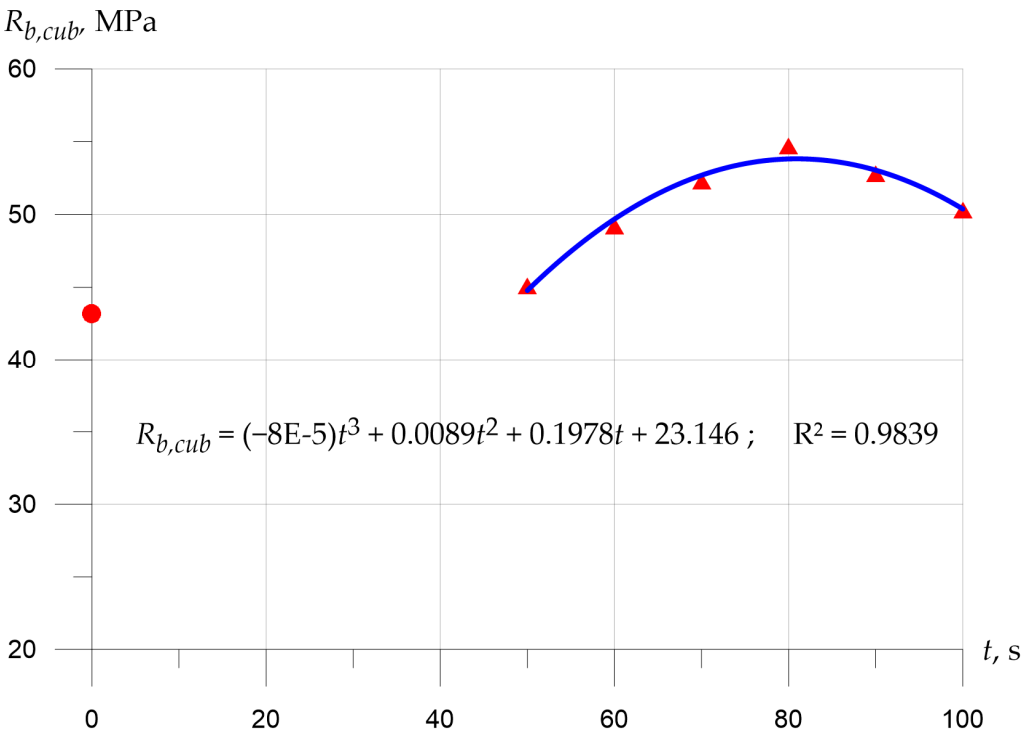

Figure 7. Dependence of the cubic compressive strength of lightweight fiber-reinforced concrete specimens on the time of treatment of CSM in VLA.

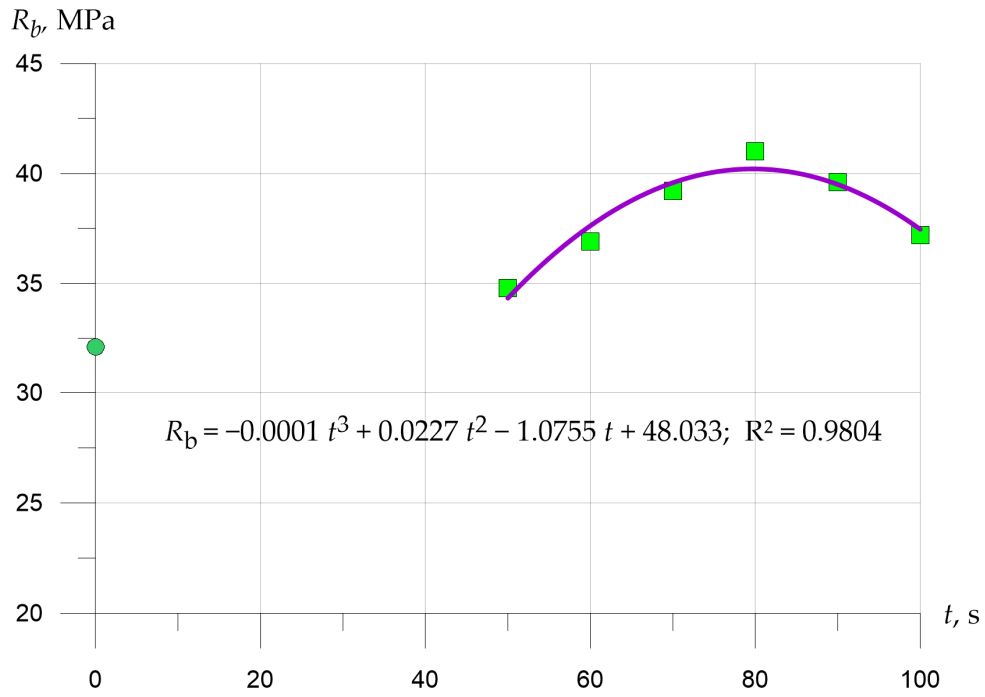

Figure 8. Dependence of the prismatic compression strength of lightweight fiber-reinforced concrete specimens on the processing time of CSM in VLA.

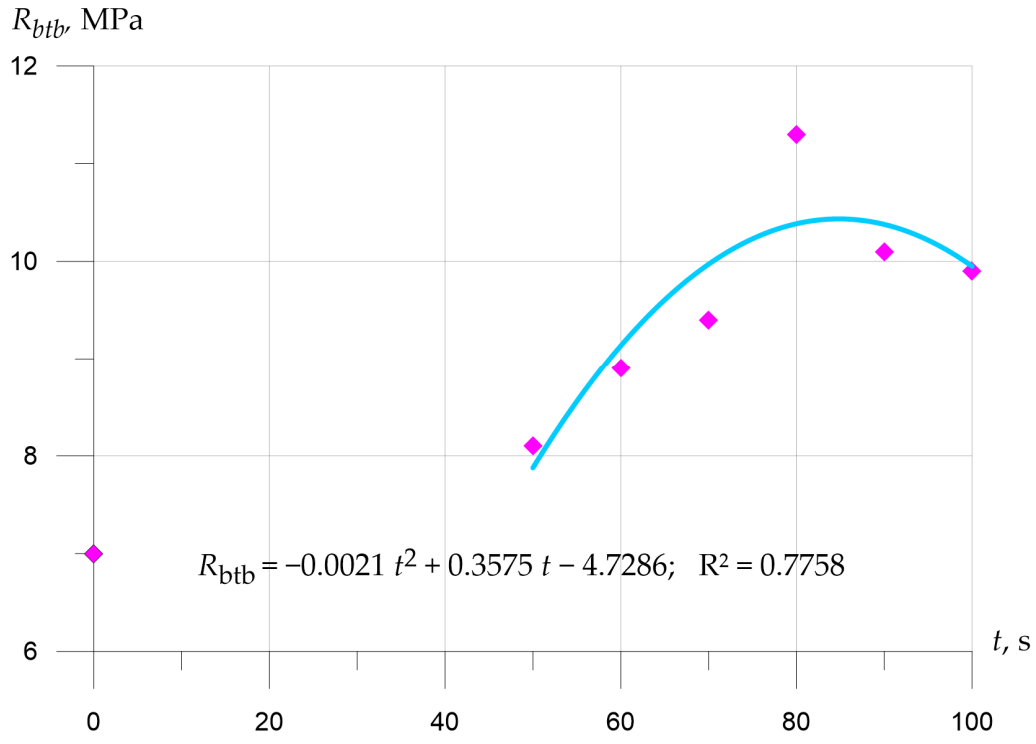

Figure 9. Dependence of the tensile strength in bending of lightweight fiber-reinforced concrete specimens on the processing time of the CSM in VLA.

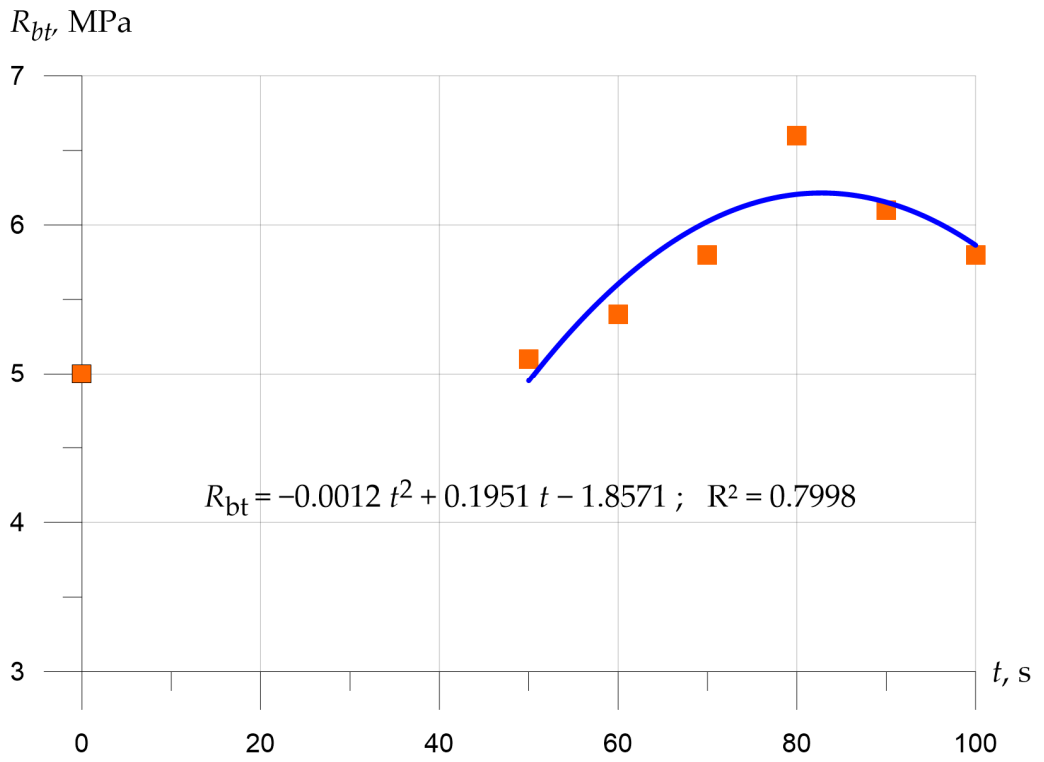

Figure 10. Dependence of the axial tensile strength of lightweight fiber-reinforced concrete specimens on the processing time of the CSM in the VLA.

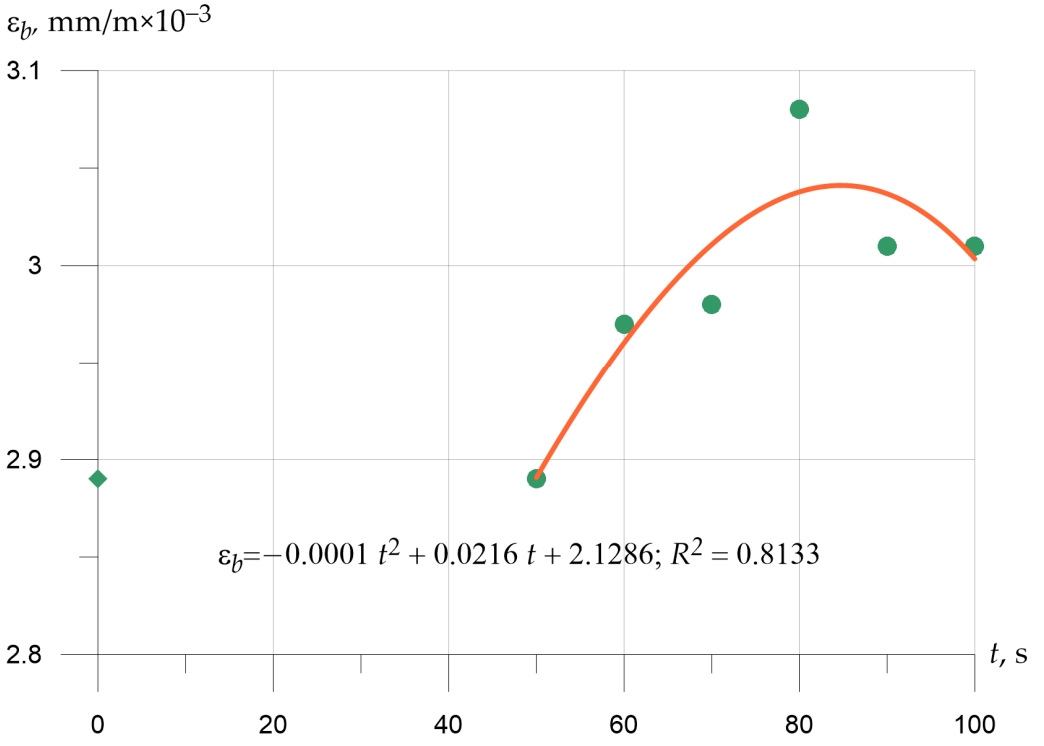

Figure 11. Dependence of ultimate deformations during axial compression of lightweight fiber-reinforced concrete specimens on the processing time of CSM in VLA.

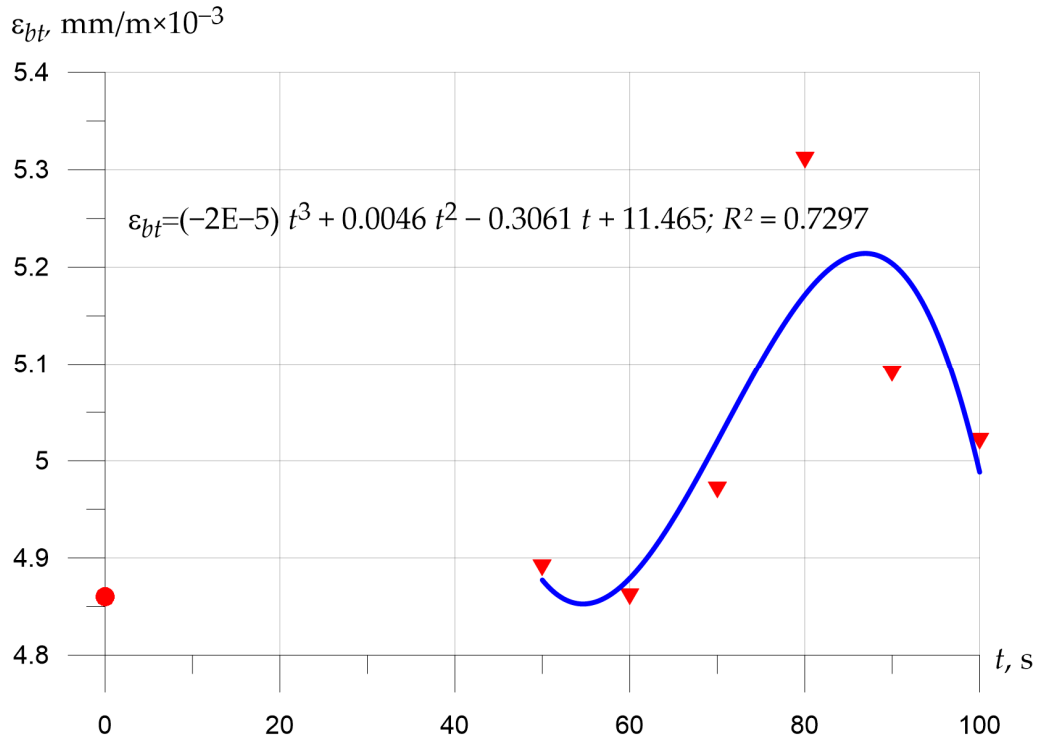

Figure 12. Dependence of ultimate deformations during axial tension of lightweight fiber-reinforced concrete specimens on the processing time of CSM in VLA.

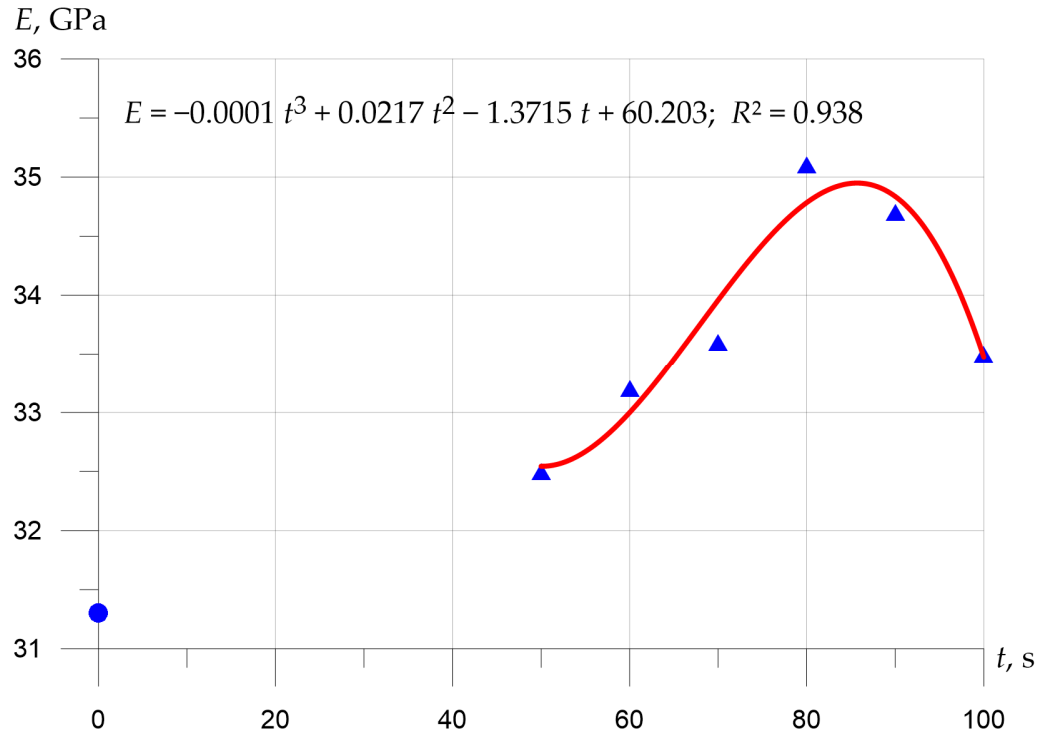

Figure 13. Dependence of the modulus of elasticity of lightweight fiber-reinforced concrete samples on the processing time of CSM in VLA.

The above values of the coefficients of determination show a good relationship between the regression curve and the data points of the processing time in the VLA and the test results.

According to the results of the experimental studies, the optimal processing time for the cement–sand mortar in the VLA apparatus is 75–85 s.

In studies [6–9,18,19,31–33], activated cement, or activated mortar part was intended for heavy concrete and aerated concrete; in particular, this is shown in the works of the authors of the scientific school under the leadership of A.I. Shuyskiy [34]. Our research is based on some of the results obtained by these authors and develops it in the direction of new types of technology and materials.

To assess the efficiency and rationality of our proposed solutions, we will compare our results with the results obtained earlier by other authors. This article defines an effective technology and electromagnetic activation parameters in the vortex layer devices of lightweight fiber-reinforced concrete components. In comparison with previous works [31–34], it was found that even a short activation time of 75–85 s leads to a significant result. In particular, the increase in strength reaches more than 60%. This significantly exceeds the previously proposed methods [31,41,42] and has the advantage, first, for its short duration, and second, for low resource and labor costs; the efficiency of strength gain is also significantly higher. The effect is especially highlighted in relation to lightweight concrete. At the same time, we strengthened the effect by the fact that concrete has dispersed reinforcement, therefore, the proposed technology helps to increase the effect not only in strength but also in deformability, which increases the operational reliability and operational possibilities of using the improved material developed by us.

4. Conclusions

According to the results of the literature review and analysis of sources devoted to studies carried out on the topics of various types of mechanical activation of cements, it was revealed that studies aimed at increasing the strength and deformative characteristics of lightweight fiber-reinforced concrete due to the activation of a cement–sand mortar in a vortex layer apparatus have not been previously carried out.

In this regard, a working hypothesis was formulated, the basic compositions and the research program were determined. Additional studies of Portland cement were also carried out using laser particle size analysis.

Large-scale experimental studies were carried out, compositions were selected, and new samples of materials obtained for the first time were molded.

The influence of the processing time of raw concrete mixture components on the strength and deformation characteristics of lightweight fiber-reinforced concrete was studied. By means of experimental studies, the optimal time for processing the cement–sand mortar in the VLA apparatus was determined-75–85 s.

An increase in strength and an improvement in deformative characteristics of lightweight fiber-reinforced concrete due to the applied activation has been substantiated.

The values of the structural quality coefficients for all experimentally determined strength characteristics of lightweight fiber-reinforced concrete made with the use of activated cement–sand mortar were calculated. The maximum coefficient of structural quality, calculated for various types of strength, was recorded for lightweight fiber-reinforced concrete activated in the VLA for 80 s.

Author Contributions: Conceptualization, L.R.M., S.A.S., E.M.S., A.B. and A.S.; methodology, S.A.S. and E.M.S.; software, S.A.S., E.M.S., A.B. and A.S.; validation, L.R.M., S.A.S., E.M.S. and A.B.; formal analysis, S.A.S. and E.M.S.; investigation, L.R.M., S.A.S., E.M.S., A.B. and B.M.; resources, B.M.; data curation, S.A.S. and E.M.S.; writing—original draft preparation, S.A.S., E.M.S. and A.B.; writing—review and editing, S.A.S., E.M.S. and A.B.; visualization, S.A.S., E.M.S., A.B. and A.S.; supervision, L.R.M. and B.M.; project administration, L.R.M. and B.M.; funding acquisition, A.B. and B.M. All authors have read and agreed to the published version of the manuscript.

Funding: The APC was funded by Don State Technical University.

Institutional Review Board Statement: Not applicable.

Informed Consent Statement: Not applicable.

Data Availability Statement: The study did not report any data.

Acknowledgments: The authors would like to acknowledge the administration of Don State Technical University for their resources and financial support.

Conflicts of Interest: The authors declare no conflict of interest. The funders had no role in the design of the study; in the collection, analyses, or interpretation of data; in the writing of the manuscript; or in the decision to publish the results.

References

1. Palmero, P.; Formia, A.; Tulliani, J.-M.; Antonaci, P. Valorisation of alumino-silicate stone muds: From wastes to source materials for innovative alkali-activated materials. *Cem. Concr. Compos.* **2017**, *83*, 251–262. [CrossRef]
2. Coppola, B.; Tulliani, J.-M.; Antonaci, P.; Palmero, P. Role of Natural Stone Wastes and Minerals in the Alkali Activation Process: A Review. *Materials* **2020**, *13*, 2284. [CrossRef] [PubMed]
3. Gado, R.A.; Hebda, M.; Łach, M.; Mikuła, J. Alkali Activation of Waste Clay Bricks: Influence of The Silica Modulus, SiO_2/Na_2O, H_2O/Na_2O Molar Ratio, and Liquid/Solid Ratio. *Materials* **2020**, *13*, 383. [CrossRef] [PubMed]
4. Humad, A.M.; Habermehl-Cwirzen, K.; Cwirzen, A. Effects of Fineness and Chemical Composition of Blast Furnace Slag on Properties of Alkali-Activated Binder. *Materials* **2019**, *12*, 3447. [CrossRef] [PubMed]
5. Roviello, G.; Ricciotti, L.; Molino, A.J.; Menna, C.; Ferone, C.; Asprone, D.; Cioffi, R.; Ferrandiz-Mas, V.; Russo, P.; Tarallo, O. Hybrid Fly Ash-Based Geopolymeric Foams: Microstructural, Thermal and Mechanical Properties. *Materials* **2020**, *13*, 2919. [CrossRef] [PubMed]
6. Kim, T.; Kang, C. Investigation of the Effect of Mixing Time on the Mechanical Properties of Alkali-Activated Cement Mixed with Fly Ash and Slag. *Materials* **2021**, *14*, 2301. [CrossRef] [PubMed]
7. Aiken, T.A.; Kwasny, J.; Sha, W.; Tong, K.T. Mechanical and durability properties of alkali-activated fly ash concrete with increasing slag content. *Constr. Build. Mater.* **2021**, *301*, 124330. [CrossRef]
8. Palankar, N.; Mithun, B.M.; Ravi Shankar, A.U. Alkali Activated Concrete with Steel Slag Aggregate for Concrete Pavement. *Int. J. Eng. Technol.* **2018**, *7*, 818–822. [CrossRef]
9. Ruengsillapanun, K.; Udtaranakron, T.; Pulngern, T.; Tangchirapat, W.; Jaturapitakkul, C. Mechanical properties, shrinkage, and heat evolution of alkali activated fly ash concrete. *Constr. Build. Mater.* **2021**, *299*, 123954. [CrossRef]
10. Sadique, M.; Al-Nageima, H.; Athertona, W.; Setonb, L.; Dempsterb, N. Mechano-chemical activation of high-Ca fly ash by cement free blending and gypsum aided grinding. *Constr. Build. Mater.* **2013**, *43*, 480–489. [CrossRef]
11. Adresi, M.; Tulliani, J.-M.; Lacidogna, G.; Antonaci, P. A Novel Life Prediction Model Based on Monitoring Electrical Properties of Self-Sensing Cement-Based Materials. *Appl. Sci.* **2021**, *11*, 5080. [CrossRef]
12. Adresi, M.; Hassani, A.; Tulliani, J.-M.; Lacidogna, G.; Antonaci, P. A study of the main factors affecting the performance of self-sensing concrete. *Adv. Cem. Res.* **2017**, *29*, 216–226. [CrossRef]
13. Adresi, M.; Hassani, A.; Javadian, S.; Tulliani, J.-M. Determining the Surfactant Consistent with Concrete in order to Achieve the Maximum Possible Dispersion of Multiwalled Carbon Nanotubes in Keeping the Plain Concrete Properties. *J. Nanotechnol.* **2016**, *2016*, 2864028. [CrossRef]
14. Benzerzour, M.; Amar, M.; Abriak, N.-E. New experimental approach of the reuse of dredged sediments in a cement matrix by physical and heat treatment. *Constr. Build. Mater.* **2017**, *140*, 432–444. [CrossRef]
15. dos Santos Vazzoler, J.; Vieira, G.L.; Teles, C.R.; Degen, M.K.; Teixeira, R.A. Investigation of the potential use of waste from ornamental stone processing after heat treatment for the production of cement-based paste. *Constr. Build. Mater.* **2018**, *177*, 314–321. [CrossRef]
16. Klos, J.; Wawrzynczak, A.; Nicholson, J.W.; Nowak, I.; Czarnecka, B. The Effect Of Heat Treatment Of An Ionomer Glass On Its Surface Characteristics And Cement-Forming Properties. *Ceram. Silik* **2020**, *64*, 1–6. [CrossRef]
17. Travush, V.I.; Karpenko, N.I.; Erofeev, V.T.; Erofeeva, I.V.; Maksimova, I.N.; Kondrashchenko, V.I.; Kesariyskiy, A.G. Investigation of powder-activated concretes by laser interferometry methods. *Constr. Mater.* **2020**, *4–5*, 18–28. [CrossRef]
18. Fedyuk, R.S.; Mochalov, A.V.; Lesovik, V.S. Modern methods of activating a binder and concrete mixtures (review). *FSAEIHE Far East. Fed. Univ. (FEFU)* **2018**, *4*, 85–99. [CrossRef]
19. Dmitrieva, M.; Leitsin, V.; Sharanova, A. Computer simulation of the strength processes of mechanically activated concrete mixtures. *AIP Conf. Proc.* **2019**, *2167*, 020072. [CrossRef]
20. Fediuk, R.S. Mechanical activation of construction binder materials by various mills. *IOP Conf. Ser. Mater. Sci. Eng.* **2016**, *125*, 012019. [CrossRef]
21. Bergold, S.T.; Goetz-Neunhoeffer, F.; Neubauer, J. Mechanically activated alite: New insights into alite hydration. *Cem. Concr. Res.* **2015**, *76*, 202–211. [CrossRef]
22. Gurevich, B.I.; Kalinkina, E.V.; Kalinkin, A.M. Binding Properties of Mechanically Activated Nepheline Containing Mining Waste. *Minerals* **2020**, *10*, 48. [CrossRef]
23. Kalinkin, A.M.; Krzhizhanovskaya, M.G.; Gurevich, B.I.; Kalinkina, E.V.; Tyukavkina, V.V. Hydration of mechanically activated blended cements studied by in situ X-ray diffraction. *Inorg. Mater.* **2015**, *51*, 828–833. [CrossRef]

24. Wei, B.; Zhang, Y.; Bao, S. Preparation of geopolymers from vanadium tailings by mechanical activation. *Constr. Build. Mater.* **2017**, *145*, 236–242. [CrossRef]
25. Singla, R.; Kumar, S.; Alex, T.C. Reactivity alteration of granulated blast furnace slag by mechanical activation for high volume usage in Portland slag cement. *Waste Biomass Valorization* **2020**, *11*, 2983–2993. [CrossRef]
26. Mucsi, G. Mechanical Activation of Power Station Fly Ash by Grinding: A Review. *J. Silic. Based Compos. Mater.* **2016**, *68*, 56–61.
27. Feng, Y.; Kero, J.; Yang, Q.; Chen, Q.; Engström, F.; Samuelsson, C.; Qi, C. Mechanical Activation of Granulated Copper Slag and Its Influence on Hydration Heat and Compressive Strength of Blended Cement. *Materials* **2019**, *12*, 772. [CrossRef]
28. Bouaziz, A.; Hamzaoui, R.; Guessasma, S.; Lakhal, R.; Achoura, D.; Leklou, N. Efficiency of high energy over conventional milling of granulated blast furnace slag powder to improve mechanical performance of slag cement paste. *Powder Technol.* **2017**, *308*, 37–46. [CrossRef]
29. Paaver, P.; Paiste, P.; Liira, M.; Kirsimäe, K. Mechanical Activation of the Ca-Rich Circulating Fluidized Bed Combustion Fly Ash: Development of an Alternative Binder System. *Minerals* **2021**, *11*, 3. [CrossRef]
30. Kumar, S.; Mucsi, G.; Kristaly, F.; Pekker, P. Mechanical activation of fly ash and its influence on micro and nano-structural behaviour of resulting geopolymers. *Adv. Powder Technol.* **2017**, *28*, 805–813. [CrossRef]
31. Ibragimov, R.A.; Korolev, E.V.; Deberdeev, T.R.; Leksin, V.V. Durability of heavy-weight concrete with portland cement treated in apparatus of vortex layer. *Constr. Mater.* **2017**, *10*, 28–31. [CrossRef]
32. Pimenov, S.I.; Ibragimov, R.A. Influence of mineralogical composition of cement when activating it on physical-technical properties of heavy concrete. *Constr. Mater.* **2017**, *8*, 64–67. [CrossRef]
33. Guan, J.; Zhang, Y.; Yao, X.; Li, L.; Zhang, L.; Yi, J. Experimental Study on the Effect of Compound Activator on the Mechanical Properties of Steel Slag Cement Mortar. *Crystals* **2021**, *11*, 658. [CrossRef]
34. Shujskij, A.I.; Torlina, E.A.; Novozhilov, A.A.; Javrujan, K.S.; Filonov, I.A. Pat. 2553893 Russian Federation, MPK B01F 13/08, Rostov-on-Don. DSTU. N 2014119043/05; declared 12.05.2014; publ. 20.06.2015, bull. N 17. 5 p. Available online: https://patentimages.storage.googleapis.com/36/cb/53/687fc0c907f7a9/RU2553893C1.pdf (accessed on 20 November 2021).
35. Mailyan, L.R.; Beskopylny, A.N.; Meskhi, B.; Stel'makh, S.A.; Shcherban, E.M.; Ananova, O. Optimization of Composition and Technological Factors for the Lightweight Fiber-Reinforced Concrete Production on a Combined Aggregate with an Increased Coefficient of Structural Quality. *Appl. Sci.* **2021**, *11*, 7284. [CrossRef]
36. Mailyan, L.R.; Beskopylny, A.N.; Meskhi, B.; Shilov, A.V.; Stel'makh, S.A.; Shcherban, E.M.; Smolyanichenko, A.S.; El'shaeva, D. Improving the Structural Characteristics of Heavy Concrete by Combined Disperse Reinforcement. *Appl. Sci.* **2021**, *11*, 6031. [CrossRef]
37. Shcherban, E.; Prokopov, A.Y.; Stel'Makh, S.; Shuyskiy, A.I. Effect of disperse reinforcement on the structural quality factor of vibrated and centrifuged concretes on the combined aggregate. *Mater. Sci. Forum* **2019**, *974*, 283–287. [CrossRef]
38. Stelmakh, S.A.; Shuyskiy, A.I.; Shcherban, E.M.; Prokopov, A.Y. Efficiency comparison of fiber reinforcement in vibrated and centrifuged concretes at different types of the applied heavy aggregate. *MSF* **2019**, *974*, 288–292. [CrossRef]
39. GOST 10180 Concretes. Methods for Strength Determination Using Reference Specimens. Available online: http://docs.cntd.ru/document/1200100908 (accessed on 20 November 2021).
40. GOST 24452 Concretes. Methods of Prismatic, Compressive Strength, Modulus of Elasticity and Poisson's Ratio Determination. Available online: https://docs.cntd.ru/document/9056198 (accessed on 20 November 2021).
41. Beskopylny, A.; Kadomtseva, E.; Strelnikov, G.; Morgun, L.; Berdnik, Y.; Morgun, V. Model of heterogeneous reinforced fiber foam concrete in bending. *IOP Conf. Ser. Mater. Sci. Eng.* **2018**, *365*, 032023. [CrossRef]
42. Beskopylny, A.; Kadomtseva, E.; Strelnikov, G.; Berdnik, Y. Stress-strain state of reinforced bimodulus beam on an elastic foundation. *IOP Conf. Ser. Earth Environ. Sci.* **2017**, *90*, 012064. [CrossRef]